SCL^2 Decoding of eBCH Based U-UV Codes

Jingyu Lin[†‡], Li Chen[†‡], Huazi Zhang[§]
[†] School of Electronics and Information Technology, Sun Yat-sen University, Guangzhou, China
[‡] Guangdong Provincial Key Laboratory of Information Security Technology, Guangzhou, China
[§] Hangzhou Research Center, Huawei Technologies Co. Ltd., Hangzhou, China
Email: linjy228@mail2.sysu.edu.cn, chenli55@mail.sysu.edu.cn, zhanghuazi@huawei.com

2025 IEEE Information Theory Workshop (ITW) | 979-8-3315-3142-3/25/$31.00 ©2025 IEEE | DOI: 10.1109/ITW62417.2025.11240337

***Abstract*—U-UV codes are good-performing short-to-medium length channel codes constructed by several algebraic component codes. They are coupled through the (U|U+V) recursive structure. With eBCH codes as the component codes, U-UV codes can be interpreted as the generalized concatenated codes (GCCs) with inner polar codes and outer eBCH codes. With ordered statistic decoding (OSD) for the outer codes, the successive cancellation list (SCL) decoding of U-UV codes can outperform that of the cyclic redundancy check (CRC)-polar codes. But the complexity of the OSD grows exponentially with its decoding order, rendering the worst-case decoding complexity of U-UV codes being too high. This paper proposes the SCL^2 decoding of eBCH based U-UV codes, in which both the inner codes and outer codes are decoded by the SCL decoding. In particular, the eBCH outer codes are interpreted as the concatenation of a polar code and a linear transform. Consequently, it can be decoded by SCL decoding with a sub-quadratic complexity. Our simulation results show that for eBCH based U-UV codes, SCL^2 decoding can reduce the binary operations required in the existing (outer) OSD-(inner) SCL decoding by an order of magnitude, while maintain the decoding performance.**

***Index Terms*—generalized concatenated codes, short-to-medium length codes, successive cancellation list decoding, U-UV codes**

I. Introduction

The next generation communication networks will enable ultra-reliable and low-latency data transmission, in which good-performing short-to-medium length (SML) channel codes play an important role. The currently known competent SML channel codes include BCH codes [1] [2], tail-biting convolutional codes [3], cyclic redundancy check (CRC)-polar codes [4]–[6] and polarization adjusted convolutional codes [7]. Recently, U-UV codes were proposed as another good-performing SML code [8]–[11]. It is constructed by several component codes of equal length, which are called the U codes and V codes. They are coupled through the $(\mathrm{U}|\mathrm{U}+\mathrm{V})$ recursive structure. This construction is also known as Plotkin construction [12]. For simplicity, we refer to it as the U-UV construction. This construction also results in polarized subchannels, each of which conveys a component code. Rates of the component codes can be designed based on the subchannel capacity [9] [10] [13]. The U-UV codes can also be interpreted as the generalized concatenated codes (GCCs), in which the component codes and the polar codes are the outer codes and the inner codes, respectively [13]. Using BCH codes as the outer codes, their successive cancellation list (SCL) decoding performance can be better than that of the CRC-polar codes [10]. Note that under the GCC paradigm, the existing SCL decoding is referred to as the (outer) OSD-(inner) SCL decoding.

In the OSD-SCL decoding of U-UV codes, component codes are decoded by the ordered statistic decoding (OSD). It can yield a near maximum likelihood (ML) decoding performance for the component codes, while produce multiple codeword estimations. However, its complexity grows exponentially with the decoding order, leading to a high OSD-SCL decoding complexity. For this complexity, the low complexity SCL decoding of U-UV codes was proposed in [14]. It reduces the complexity of OSD by introducing an efficient skipping rule. Meanwhile, it also curbs the use of OSD through pruning the redundant SCL decoding paths. However, the sequential Gaussian elimination (GE) required by the OSD imposes an uncompromised decoding latency, affecting the practical application of U-UV codes. And the variable-dependent nature of GE's execution steps makes it hardware-unfriendly.

In order to further facilitate the decoding of U-UV codes, this paper proposes the SCL^2 decoding for the eBCH based U-UV codes, in which both the inner and outer codes are decoded by the SCL decoding. By interpreting the eBCH codes as concatenation of a polar code and a linear transform, they can be decoded by the SCL algorithm [15]. With a sufficiently large list size l, the SCL decoding can achieve a near ML decoding performance for eBCH codes with a complexity of $\mathcal{O}(l \cdot n\log_2 n)$, while the order-$\tau$ OSD has a complexity of $\mathcal{O}(k^\tau)$. Note that n and k are length and dimension of the code, respectively. Consequently, decoding complexity of U-UV codes can be significantly reduced, making the codes more practical. Note that OSD requires $\tau \geq \min\{\lfloor \frac{d}{4} \rfloor, k\}$ to approach the ML decoding performance of the outer code, where d is its minimum distance [16]. The complexity of OSD-SCL decoding grows exponentially with the length of the outer codes. Hence, SCL^2 decoding will be more suitable for U-UV codes with long outer codes. Our simulation results show that for the eBCH based U-UV codes, SCL^2 decoding can reduce the binary operations required in the existing OSD-SCL decoding by an order of magnitude, while maintain the decoding performance.

II. Preliminaries

A. U-UV *Codes*

Let the U code and V code be two linear block codes of length n with dimensions k_U and k_V, respectively. The 1-level

U-UV code of length $2n$ and dimension $k_{\mathrm{U}}+k_{\mathrm{V}}$ is constructed as [12]

$$\{(\boldsymbol{u}\,|\,\boldsymbol{u}+\boldsymbol{v}); \boldsymbol{u}\in\mathcal{C}_{\mathrm{U}}, \boldsymbol{v}\in\mathcal{C}_{\mathrm{V}}\}, \tag{1}$$

where $\mathcal{C}_{\mathrm{U}}$ and $\mathcal{C}_{\mathrm{V}}$ denote the codebooks of the U code and V code, respectively. A multi-level U-UV code can be constructed by extending this construction recursively through involving more component U codes and V codes. A γ-level U-UV code consists of $H=2^{\gamma}$ component codes. Let U_h denote the h-th component code, where $h=1,2,\cdots,H$. The component code U_h is an eBCH code of length n and rate $R_h=k_h/n$. The γ-level U-UV code has a length of Hn and a rate of $(\sum_{h=1}^{H}R_h)/H$.

In this work, eBCH codes are used as component codes, since they have a length of power of two to be decoded by the SCL algorithm. And their large minimum distances ensure the good distance properties of U-UV codes. As illustrated in Fig. 1, the U-UV codes can be interpreted as generalized eBCH-polar concatenated codes, in which H outer eBCH codes are concatenated with n inner polar codes. Rates of the outer codes can be designed by computing the finite length rate of the polarized subchannels and further applying the equal error probability rule to adjusting them [10]. With OSD for the outer codes, the OSD-SCL decoding of U-UV codes can be realized, but with an outer decoding complexity that is exponential in nature [10].

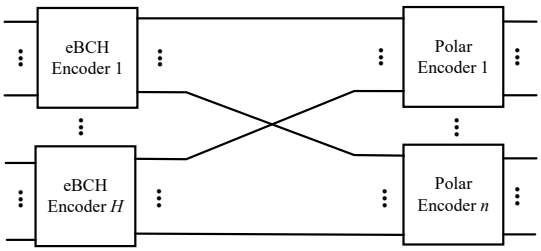

Fig. 1. GCC interpretation of a U-UV code with eBCH component codes.

B. SCL Decoding of Binary Linear Block Codes

Let $\mathbb{F}_2$ denote the binary field and $\mathbb{F}_{2^m}$ further denote the nonbinary field of characteristic two and with a primitive element α. Let $\mathbf{F}=((1,0),(1,1))^{\mathrm{T}}$ denote the Arıkan kernel. A polar code of length $n=2^m$ and dimension k is a linear block code defined by the generator matrix $\mathbf{G}_{\mathrm{p}}=\mathbf{F}^{\otimes m}\in\mathbb{F}_2^{n\times n}$, where $\otimes m$ denotes the m-fold Kronecker product. Note that $\mathbf{G}_{\mathrm{p}}$ is invertible, which implies that any $(n=2^m,k)$ binary linear block code $\mathcal{C}$ with a generator matrix $\mathbf{G}\in\mathbb{F}_2^{k\times n}$ can be obtained as an appropriate subspace of the codebook defined by $\mathbf{G}_{\mathrm{p}}$ [17]. The codebook $\mathcal{C}$ can be defined as

$$\begin{aligned}\mathcal{C}&\triangleq\{\boldsymbol{c}=\boldsymbol{m}\mathbf{G}\,|\,\forall\boldsymbol{m}\in\mathbb{F}_2^k\}\\&=\{\boldsymbol{c}=\boldsymbol{m}(\mathbf{G}\mathbf{G}_{\mathrm{p}}^{-1})\mathbf{G}_{\mathrm{p}}\,|\,\forall\boldsymbol{m}\in\mathbb{F}_2^k\}\\&=\{\boldsymbol{c}=\boldsymbol{x}\mathbf{G}_{\mathrm{p}}\,|\,\boldsymbol{x}=\boldsymbol{m}\mathbf{G}\mathbf{G}_{\mathrm{p}}^{-1},\forall\boldsymbol{m}\in\mathbb{F}_2^k\}.\end{aligned} \tag{2}$$

Hence, its codeword $\boldsymbol{c}$ can be reinterpreted as a polar codeword. $\mathcal{C}$ can also be regarded as a polar code concatenated with a linear transform defined by $\mathbf{G}\mathbf{G}_{\mathrm{p}}^{-1}$. To facilitate the successive cancellation (SC) decoding of $\mathcal{C}$, GE shall be performed on $\mathbf{G}\mathbf{G}_{\mathrm{p}}^{-1}$, obtaining $\mathbf{M}=\mathbf{E}\mathbf{G}\mathbf{G}_{\mathrm{p}}^{-1}\in\mathbb{F}_2^{k\times n}$, where $\mathbf{M}$ is a matrix of row reduced echelon form and $\mathbf{E}$ is an elimination matrix. The codeword $\boldsymbol{c}$ can be represented as

$$\boldsymbol{c}=\boldsymbol{m}_{\mathrm{p}}\mathbf{M}\mathbf{G}_{\mathrm{p}}, \tag{3}$$

where $\boldsymbol{m}_{\mathrm{p}}=\boldsymbol{m}\mathbf{E}^{-1}\in\mathbb{F}_2^k$ is the transformed information vector. With $\boldsymbol{m}_{\mathrm{p}}$ as the information vector of the polar code, $\boldsymbol{x}=\boldsymbol{m}_{\mathrm{p}}\mathbf{M}$ consists of k information bits and $n-k$ frozen bits. The information bits are indexed by the pivot columns of $\mathbf{M}$. They constitute the information set $\mathcal{A}$. The frozen bits are linear combination of the information bits of lower indices. Hence, $\mathcal{C}$ can now be regarded as a polar code with dynamic frozen bits [17]. The SC decoding can be performed to obtain the information vector estimation $\hat{\boldsymbol{m}}_{\mathrm{p}}$. The original information vector $\boldsymbol{m}$ can be further estimated by $\hat{\boldsymbol{m}}=\hat{\boldsymbol{m}}_{\mathrm{p}}\mathbf{E}$.

Let $P_{\mathrm{e}}(\mathcal{W}_i)$ denote the error probability on the i-th polarized subchannel of a length-n polar code, where $1\le i\le n$. The union bound on the block error rate (BLER) of SC decoding is [4]

$$P_{\text{block}}\le\sum_{i\in\mathcal{A}}P_{\mathrm{e}}(\mathcal{W}_i), \tag{4}$$

where $P_{\mathrm{e}}(\mathcal{W}_i)$ can be computed via Monte Carlo simulation or Gaussian approximation (GA) [13] [18]–[20]. Therefore, the SC decoding performance of $\mathcal{C}$ depends on the selection of information set $\mathcal{A}$. Since $\mathcal{A}$ is not constituted by the indices of subchannels with the smallest error probability, the SC decoding performance of $\mathcal{C}$ can be worse than that of a well-designed polar code.

In order to improve the SC decoding performance, permutation matrix $\mathbf{P}\in\mathbb{F}_2^{n\times n}$ was introduced in [15] to adjust the information set $\mathcal{A}$. The codebook $\mathcal{C}$ can be rewritten as

$$\begin{aligned}\mathcal{C}&\triangleq\{\boldsymbol{c}=\boldsymbol{m}\mathbf{G}\,|\,\forall\boldsymbol{m}\in\mathbb{F}_2^k\}\\&=\{\boldsymbol{c}=\boldsymbol{m}(\mathbf{G}\mathbf{P}^{-1}\mathbf{G}_{\mathrm{p}}^{-1})\mathbf{G}_{\mathrm{p}}\mathbf{P}\,|\,\forall\boldsymbol{m}\in\mathbb{F}_2^k\}\\&=\{\boldsymbol{c}=\boldsymbol{m}\mathbf{E}^{-1}(\mathbf{E}\mathbf{G}\mathbf{P}^{-1}\mathbf{G}_{\mathrm{p}}^{-1})\mathbf{G}_{\mathrm{p}}\mathbf{P}\,|\,\forall\boldsymbol{m}\in\mathbb{F}_2^k\}\\&=\{\boldsymbol{c}=(\boldsymbol{m}_{\mathrm{p}}\mathbf{M}\mathbf{G}_{\mathrm{p}})\mathbf{P}\,|\,\forall\boldsymbol{m}_{\mathrm{p}}\in\mathbb{F}_2^k\},\end{aligned} \tag{5}$$

where the elimination matrix $\mathbf{E}$ transforms $\mathbf{G}\mathbf{P}^{-1}\mathbf{G}_{\mathrm{p}}^{-1}$ into the row reduced echelon form, and $\mathbf{M}=\mathbf{E}\mathbf{G}\mathbf{P}^{-1}\mathbf{G}_{\mathrm{p}}^{-1}$. With this transform, any codeword of $\mathcal{C}$ can be seen as a permuted codeword of a polar code. Information set $\mathcal{A}$ can be adjusted by different permutation matrices $\mathbf{P}$. Theoretically, a permutation matrix that minimizes P_{block} should be chosen. Subsequently, with an adequate list size, the SCL decoding can achieve a near ML decoding performance for $\mathcal{C}$. Fig. 2 summarizes the SCL decoding described above.

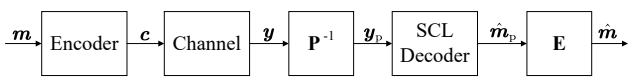

Fig. 2. Block diagram of the SCL decoding of binary linear block codes.

III. SCL^2 Decoding

A. Permutation Matrix for SCL Decoding of eBCH Codes

For SCL decoding of eBCH codes, permutation matrix $\mathbf{P}$ can be constructed to ensure a good decoding performance. Consider the $(n = 2^m, k)$ eBCH code with a generator matrix $\mathbf{G} \in \mathbb{F}_2^{k\times n}$. Let $\mathbf{P}_{a,b}$ denote the row-a column-b entry of $\mathbf{P} \in \mathbb{F}_2^{n\times n}$, where $0 \le a, b \le n-1$. It can be defined as

$$\mathbf{P}_{a,b} = \begin{cases} 1, & \text{if } \alpha^a = \sum_{j=0}^{m-1} u_j \cdot \alpha^j, b = \sum_{j=0}^{m-1} u_j \cdot 2^j, \\ & 0 \le a \le n-2 \text{ or } a = n-1, b = 0; \\ 0, & \text{otherwise}, \end{cases} \tag{6}$$

where coefficients $u_0, u_1, \cdots, u_{m-1} \in \mathbb{F}_2$. This design ensures that the first few columns of $\mathbf{G}\mathbf{P}^{-1}\mathbf{G}_{\mathrm{p}}^{-1}$ are zero vectors. Subsequently, the first few columns of $\mathbf{M} = \mathbf{E}\mathbf{G}\mathbf{P}^{-1}\mathbf{G}_{\mathrm{p}}^{-1}$ are also zero vectors. It implies that the polarized subchannels with low indices of the polar code (transformed from the eBCH code) convey frozen bits. In general, the error probability on these subchannels are relatively large. This permutation matrix aims to optimize the SC decoding BLER P_{block}, but it can not guarantee it being minimized. The following example demonstrates the transformation of an eBCH code and the upper bound of its SC decoding BLER.

Example 1. Let us consider the $(16, 5)$ eBCH code with a generator matrix $\mathbf{G}$. With the permutation matrix $\mathbf{P}$ defined as in (6) and $\mathbf{G}_{\mathrm{p}} = \mathbf{F}^{\otimes 4}$, one can obtain

$$\mathbf{G}\mathbf{P}^{-1}\mathbf{G}_{\mathrm{p}}^{-1} = \begin{bmatrix} 0&0&0&0&0&0&0&1&0&0&0&0&0&0&0&0 \\ 0&0&0&0&0&0&0&0&0&0&0&0&0&0&1&0 \\ 0&0&0&0&0&0&0&0&0&0&0&0&0&1&1&1 \\ 0&0&0&0&0&0&0&0&0&0&0&1&0&1&1&0 \\ 0&0&0&0&0&0&0&1&0&0&0&1&0&1&1&1 \end{bmatrix}. \tag{7}$$

The first seven columns of $\mathbf{G}\mathbf{P}^{-1}\mathbf{G}_{\mathrm{p}}^{-1}$ are zeros vectors. By performing GE on $\mathbf{G}\mathbf{P}^{-1}\mathbf{G}_{\mathrm{p}}^{-1}$, $\mathbf{M}$ can be obtained as

$$\mathbf{M} = \begin{bmatrix} 0&0&0&0&0&0&0&1&0&0&0&0&0&0&0&0 \\ 0&0&0&0&0&0&0&0&0&0&0&1&0&0&0&0 \\ 0&0&0&0&0&0&0&0&0&0&0&0&0&1&0&0 \\ 0&0&0&0&0&0&0&0&0&0&0&0&0&0&1&0 \\ 0&0&0&0&0&0&0&0&0&0&0&0&0&0&0&1 \end{bmatrix}. \tag{8}$$

Indices of the weight-1 columns of $\mathbf{M}$ constitute the information set of the transformed polar code, i.e., $\mathcal{A} = \{8, 12, 14, 15, 16\}$. When transmitted over the additive white Gaussian noise (AWGN) channel at the signal-to-noise ratio (SNR) of 2.5 dB, the upper bound of SC decoding BLER is 0.269 according to (4).

B. Interaction Between Inner and Outer SCL Decoding

The SCL^2 decoder of a γ-level U-UV code consists of n inner SCL decoders and $H = 2^\gamma$ outer SCL decoders, as shown in Fig. 3. Assume that a U-UV codeword $\boldsymbol{c} = (c_1, c_2, \cdots, c_{Hn}) \in \mathbb{F}_2^{Hn}$ is transmitted through a discrete memoryless channel using binary phase shift keying (BPSK) modulation of mapping: $0 \mapsto 1; 1 \mapsto -1$. Let $\boldsymbol{y} = (y_1, y_2, \cdots, y_{Hn}) \in \mathbb{R}^{Hn}$ denote the received symbol vector

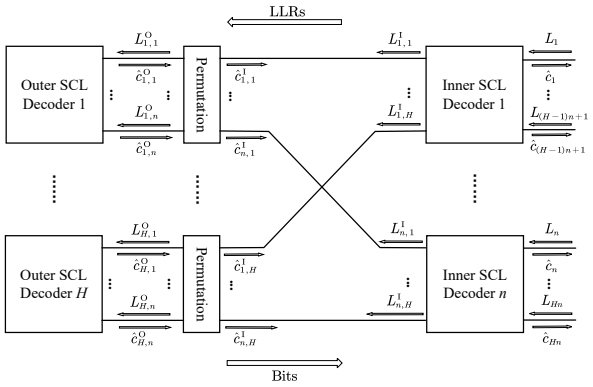

Fig. 3. SCL^2 decoding of a γ-level U-UV codes.

and $\boldsymbol{L} = (L_1, L_2, \cdots, L_{Hn}) \in \mathbb{R}^{Hn}$ denote the corresponding log-likelihood ratio (LLR) vector with entries defined as

$$L_j = \ln \frac{p(y_j|c_j = 0)}{p(y_j|c_j = 1)}, \tag{9}$$

where $j = 1, 2, \cdots, Hn$. These LLRs are partitioned into n groups, each of which is the input of an inner SCL decoder. In particular, input of the t-th inner SCL decoder is

$$L_t, L_{n+t}, \cdots, L_{(H-1)n+t}, \tag{10}$$

where $t = 1, 2, \cdots, n$. In the following description, the superscript I and O in the symbols indicate that they are symbols of the inner and outer decoders, respectively. At the beginning, all the n inner SCL decoders compute the LLRs of the first subchannels of the inner polar codes [21], which constitute

$$\boldsymbol{L}^{\mathrm{I}}_{-,1} = (L^{\mathrm{I}}_{1,1}, L^{\mathrm{I}}_{2,1}, \cdots, L^{\mathrm{I}}_{n,1}). \tag{11}$$

By further performing the permutation $\mathbf{P}^{-1}$, they form the input LLR vector for the first outer SCL decoder as:

$$\boldsymbol{L}^{\mathrm{O}}_1 = (L^{\mathrm{O}}_{1,1}, L^{\mathrm{O}}_{1,2}, \cdots, L^{\mathrm{O}}_{1,n}) = \boldsymbol{L}^{\mathrm{I}}_{-,1}\mathbf{P}^{-1}. \tag{12}$$

In the SCL^2 decoding with a list size of l, the first outer SCL decoder produces l codeword estimations. They are denoted as:

$$\hat{\boldsymbol{c}}^{\mathrm{O}}_1(s) = (\hat{c}^{\mathrm{O}}_{1,1}(s), \hat{c}^{\mathrm{O}}_{1,2}(s), ..., \hat{c}^{\mathrm{O}}_{1,n}(s)), \tag{13}$$

where $s = 1, 2, \cdots, l$. After applying the permutation $\mathbf{P}$, they are fed back to the inner SCL decoders as:

$$\hat{\boldsymbol{c}}^{\mathrm{I}}_{-,1}(s) = (\hat{c}^{\mathrm{I}}_{1,1}(s), \hat{c}^{\mathrm{I}}_{2,1}(s), \cdots, \hat{c}^{\mathrm{I}}_{n,1}(s)) = \hat{\boldsymbol{c}}^{\mathrm{O}}_1(s)\mathbf{P}. \tag{14}$$

With $\hat{c}^{\mathrm{I}}_{t,1}(s)$ as the bit estimation of the first subchannel, the t-th inner SCL decoder computes $L^{\mathrm{I}}_{t,2}(s)$ for the second subchannel. Grouping the LLRs of the second subchannels of the inner polar codes, one can obtain

$$\boldsymbol{L}^{\mathrm{I}}_{-,2}(s) = (L^{\mathrm{I}}_{1,2}(s), L^{\mathrm{I}}_{2,2}(s), \cdots, L^{\mathrm{I}}_{n,2}(s)), \tag{15}$$

where $s = 1, 2, \cdots, l$. The input LLR vectors for next outer SCL decoder are further formed by $\boldsymbol{L}^{\mathrm{O}}_2(s) = \boldsymbol{L}^{\mathrm{I}}_{-,2}(s)\mathbf{P}^{-1}$.

Based on each LLR input, the outer SCL decoder produces l codeword estimations. Hence, as the outer codes are decoded, the number of decoding paths increases exponentially, leading

to an exponentially growing complexity. In order to reduce the decoding complexity, only the l most likely estimations will be reserved for each outer code. That says an l^2-to-l decoding path pruning will be performed after each outer SCL decoding except the first one. Let

$$\boldsymbol{L}_h^{\mathrm{O}}(s) = (L_{h,1}^{\mathrm{O}}(s), L_{h,2}^{\mathrm{O}}(s), \cdots, L_{h,n}^{\mathrm{O}}(s)) \tag{16}$$

denote the s-th input vector for the h-th outer SCL decoder, where $h = 2, 3, ..., H$. Further let

$$\hat{\boldsymbol{c}}_h^{\mathrm{O}}(s, s') = (\hat{c}_{h,1}^{\mathrm{O}}(s, s'), \hat{c}_{h,2}^{\mathrm{O}}(s, s'), \cdots, \hat{c}_{h,n}^{\mathrm{O}}(s, s')) \tag{17}$$

denote the s'-th codeword estimation produced by the h-th outer SCL decoder with $\boldsymbol{L}_h^{\mathrm{O}}(s)$ as the input, where $s' = 1, 2, \cdots, l$. The correlation distance between $\boldsymbol{L}_h^{\mathrm{O}}(s)$ and $\hat{\boldsymbol{c}}_h^{\mathrm{O}}(s, s')$ is defined as

$$\begin{aligned} \lambda_h^{(s,s')} &= \lambda(\boldsymbol{L}_h^{\mathrm{O}}(s), \hat{\boldsymbol{c}}_h^{\mathrm{O}}(s, s')) \\ &= \sum_{j \in \Psi_h^{(s,s')}} |L_{h,j}^{\mathrm{O}}(s)|, \end{aligned} \tag{18}$$

where $\Psi_h^{(s,s')} = \{j | L_{h,j}^{\mathrm{O}}(s) \cdot (1 - 2\hat{c}_{h,j}^{\mathrm{O}}(s, s')) < 0\}$. It is used as the metric for assessing the likelihood of the codeword estimations. A smaller correlation distance indicates the estimation is more likely to be the transmitted codeword. The accumulated correlation distance (ACD) corresponding to $\hat{\boldsymbol{c}}_h^{\mathrm{O}}(s, s')$ is defined as

$$\Phi_h^{(s,s')} = \Phi_{h-1}^{(s)} + \lambda_h^{(s,s')}, \tag{19}$$

where $\Phi_{h-1}^{(s)}$ is the ACD of the s-th decoding path corresponding to $\hat{\boldsymbol{c}}_{h-1}^{\mathrm{O}}(s)$. At the beginning, $\Phi_1^{(s)}$ was initialized as

$$\Phi_1^{(s)} = \lambda_1^{(s)}, \tag{20}$$

where $\lambda_1^{(s)} = \lambda(\boldsymbol{L}_1^{\mathrm{O}}, \hat{\boldsymbol{c}}_1^{\mathrm{O}}(s))$ is the correlation distance between the input LLR vector $\boldsymbol{L}_1^{\mathrm{O}}$ of the first outer SCL decoder and its s-th codeword estimations $\hat{\boldsymbol{c}}_1^{\mathrm{O}}(s)$. A decoding path that yields a smaller ACD is more likely to be the correct path. Therefore, the l^2-to-l decoding path pruning select the l decoding paths that yield the l smallest ACDs. These ACDs are relabeled as $\Phi_h^{(1)}, \Phi_h^{(2)}, \cdots, \Phi_h^{(l)}$. Their corresponding codeword estimations are relabeled as $\hat{\boldsymbol{c}}_h^{\mathrm{O}}(1), \hat{\boldsymbol{c}}_h^{\mathrm{O}}(2), \cdots, \hat{\boldsymbol{c}}_h^{\mathrm{O}}(l)$, respectively. The feedback for inner SCL decoders are further obtained by performing permutation $\mathbf{P}$ on them.

After the H-th outer SCL decoding, there remain l decoding paths that yield $\Phi_H^{(1)}, \Phi_H^{(2)}, \cdots, \Phi_H^{(l)}$. Let

$$s^* = \arg\min\{\Phi_H^{(s)}, s = 1, 2, \cdots, l\}. \tag{21}$$

The decoding path that yields $\Phi_H^{(s^*)}$ corresponds to the most likely codeword estimation under this decoding. The estimated U-UV codeword $\hat{\boldsymbol{c}}$ can be reconstructed by coupling $\hat{\boldsymbol{c}}_1^{\mathrm{I}}(s^*), \hat{\boldsymbol{c}}_2^{\mathrm{I}}(s^*), \cdots, \hat{\boldsymbol{c}}_n^{\mathrm{I}}(s^*)$ as in (1).

Algorithm 1 summarizes the above decoding process. In general, the inner SCL decoders provide LLR vectors for the outer SCL decoders. The outer SCL decoders return component codeword estimations to the inner SCL decoders. The SCL^2 decoding is realized by such an information exchange mechanism between the inner and outer SCL decoders.

Algorithm 1: SCL^2 Decoding of U-UV Codes

Input: $\boldsymbol{L}$;
Output: $\hat{\boldsymbol{c}}$;
For $t = 1, 2, \cdots, n$ **do**
  Perform LLR update of the t-th inner SCL decoder, yielding $L_{t,1}^{\mathrm{I}}$;
Obtain $\boldsymbol{L}_1^{\mathrm{O}}$ as in (12);
Perform SCL decoding of the first outer code, yielding $\{\hat{\boldsymbol{c}}_1^{\mathrm{O}}(s) | s = 1, 2, \cdots, l\}$;
Determine $\Phi_1^{(s)}$ as in (20) ;
Perform permutation $\mathbf{P}$ on each estimation candidate of $\{\hat{\boldsymbol{c}}_1^{\mathrm{O}}(s) | s = 1, 2, \cdots, l\}$;
For $h = 2, 3, \cdots, H$ **do**
  For $t = 1, 2, \cdots, n$ **do**
    Perform LLR update of the t-th inner SCL decoder, yielding $\{L_{t,h}^{\mathrm{I}}(s) | s = 1, 2, \cdots, l\}$;
  For $s = 1, 2, \cdots, l$ **do**
    Perform permutation $\mathbf{P}^{-1}$ on $\boldsymbol{L}_{-,h}^{\mathrm{I}}(s)$, yielding $\boldsymbol{L}_h^{\mathrm{O}}(s)$;
  Perform SCL decoding of the h-th outer code, yielding $\{\hat{\boldsymbol{c}}_h^{\mathrm{O}}(s, s') | s, s' = 1, 2, \cdots, l\}$;
  Determine $\Phi_h^{(s,s')}$ as in (18) and (19) ;
  Select the l estimations with the smallest $\Phi_h^{(s,s')}$ and relabel them as $\{\hat{\boldsymbol{c}}_h^{\mathrm{O}}(s) | s = 1, 2, \cdots, l\}$;
  Perform permutation $\mathbf{P}$ on each estimation candidate of $\{\hat{\boldsymbol{c}}_h^{\mathrm{O}}(s) | s = 1, 2, \cdots, l\}$;
Select the most likely decoding path as in (21) ;
Reconstruct $\hat{\boldsymbol{c}}$ as in (1);

C. Complexity Analysis

In the proposed SCL^2 decoding, the complexity attributes to the LLR updates and the decoding path sorting of both the inner and outer SCL decoders.

With a list size of l, complexity of the LLR updates of the inner SCL decoders is $\mathcal{O}(nlH\log_2 H)$. Moreover, complexity of the decoding path sorting of the inner SCL decoders is $\mathcal{O}(Hl^2\log_2 l)$. If the list size of the h-th outer SCL decoder is l_h, complexity of its LLR updates is $\mathcal{O}(l_h n\log_2 n)$, and complexity of its path sorting is $\mathcal{O}(k_h l_h \log_2 l_h)$. Note that k_h is the dimension of the outer code. And $l_h \geq l$ should be satisfied since the outer SCL decoder needs to produce l codeword estimations for the inner SCL decoders. Considering there are H outer codes, complexity of the LLR updates of the outer SCL decoding is $\mathcal{O}(\sum_{h=1}^{H} l_h n\log_2 n)$. Similarly, complexity of the decoding path sorting of the outer SCL decoding is $\mathcal{O}(\sum_{h=1}^{H} k_h l_h \log_2 l_h)$.

Table I summarizes the above analysis, which also shows the existing OSD-SCL decoding complexity of U-UV codes. In the OSD-SCL decoding, the h-th outer code is decoded by an order-τ_h OSD. It can be seen that the proposed SCL^2

TABLE I
DECODING COMPLEXITY COMPARISON BETWEEN SCL^2 DECODING AND OSD-SCL DECODING

	Inner LLR Update	Outer LLR Update	Inner Path Sorting	Outer Path Sorting	OSD
U-UV, SCL^2 (l)	$\mathcal{O}(nlH\log_2 H)$	$\mathcal{O}(\sum_{h=1}^{H} l_h n\log_2 n)$	$\mathcal{O}(Hl^2\log_2 l)$	$\mathcal{O}(\sum_{h=1}^{H} k_h l_h \log_2 l_h)$	-
U-UV, OSD-SCL (l) [10]	$\mathcal{O}(nlH\log_2 H)$	-	$\mathcal{O}(Hl^2\log_2 l)$	$\mathcal{O}(lH\Gamma^*\log_2 l)^\dagger$	$\mathcal{O}(lHk_{h^*}^{\tau_{h^*}})^\ddagger$

† $\Gamma^* = \max\{\sum_{j=0}^{\tau_h}\binom{k_h}{j} | h = 1, 2, \cdots, H\}$; ‡ $h^* = \arg\max\{k_h^{\tau_h} | h = 1, 2, \cdots, H\}$.

decoding removes the binary operations (BOPs) required by the OSD. But it incurs extra floating point operations (FLOPs) for its outer LLR updates. Moreover, OSD requires $\tau_h \geq \min\{\lfloor \frac{d_h}{4} \rfloor, k_h\}$ to approach the ML decoding performance of the h-th outer code, where d_h is its minimum distance. τ_h grows linearly with the length of the h-th outer code, implying that the complexity of OSD-SCL decoding grows exponentially with the length of the outer codes, while SCL^2 decoding exhibits sub-quadratic growth. Hence, SCL^2 decoding will be more suitable for U-UV codes with long outer codes.

IV. SIMULATION RESULTS

This section shows our simulation results on SCL^2 decoding of the eBCH based U-UV codes. They are obtained over the AWGN channel using BPSK modulation. List sizes of the outer SCL decoding and orders of the OSD are chosen such that a near ML decoding performance can be achieved for the eBCH codes. Performance of the CRC-polar codes designed by the 5-th generation new radio (5G NR) standard are also shown as benchmarks. A length-8 CRC code is employed for its CRC aided (CA)-SCL decoding.

A. Decoding Performance

Fig. 4 shows the BLER performance of the SCL^2 decoding of the 2-level $(256, 183)$ U-UV code. It is constructed by the $(64, 57)$, $(64, 51)$, $(64, 51)$ and $(64, 24)$ eBCH codes. The CA-SCL decoding performance of the $(256, 183)$ CRC-polar code is also provided. It can be seen that with the same inner SCL decoding list size, the proposed SCL^2 decoding yields a similar performance as the OSD-SCL decoding. As the SNR increases, the SCL^2 decoding can even slightly outperform the OSD-SCL decoding.

Fig. 5 shows the BLER performance of the SCL^2 decoding of the 3-level $(512, 250)$ U-UV code. It is constructed by the $(64, 57)$, $(64, 51)$, $(64, 45)$, $(64, 24)$, $(64, 45)$, $(64, 18)$, $(64, 10)$ and $(64, 0)$ eBCH codes. Note that the $(64, 0)$ outer code carries frozen bits. The CA-SCL decoding performance of the $(512, 250)$ CRC-polar code is also provided. Similarly, the SCL^2 decoding yield a similar performance as the OSD-SCL decoding.

B. Decoding Complexity

Table II compares the decoding complexity of three coding schemes, including the SCL^2 decoding of the $(512, 250)$ U-UV code, the OSD-SCL decoding of the same U-UV code and the CA-SCL decoding of the $(512, 250)$ CRC-polar code. It can be seen that the SCL^2 decoding reduces the amount of BOPs by an order of magnitude over the OSD-SCL decoding, while it incurs a slightly larger amount of FLOPs. This vindicates our theoretical analysis of section III-C. It can also be seen that the U-UV code's performance advantage over the CRC-polar code is realized at the cost of higher decoding complexity.

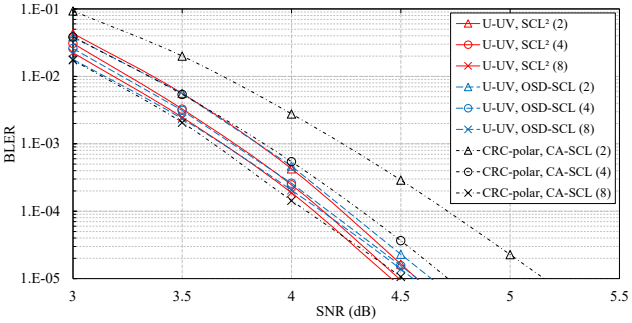

Fig. 4. SCL^2 decoding performance of the $(256, 183)$ U-UV code.

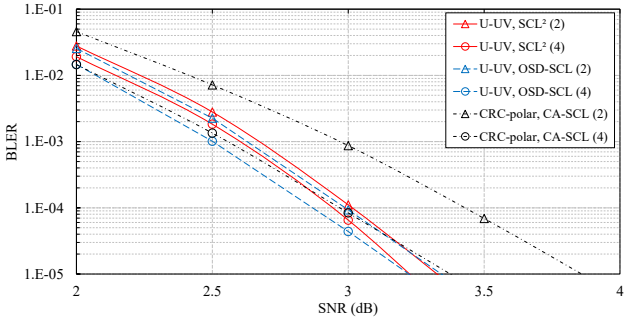

Fig. 5. SCL^2 decoding performance of the $(512, 250)$ U-UV code.

TABLE II
DECODING COMPLEXITY COMPARISON OF THREE CODING SCHEMES

Scheme	FLOPs	BOPs
U-UV, SCL^2(2)	4.06×10^5	1.10×10^5
U-UV, SCL^2(4)	8.08×10^5	2.27×10^5
U-UV, OSD-SCL(2)	2.41×10^5	1.09×10^6
U-UV, OSD-SCL(4)	5.20×10^5	2.14×10^6
CRC-polar, CA-SCL(2)	1.03×10^4	3.46×10^3
CRC-polar, CA-SCL(4)	2.12×10^4	6.56×10^3

ACKNOWLEDGEMENTS

This work is supported in part by the National Natural Science Foundation of China (NSFC) with grant ID 62471503 and in part by the Natural Science Foundation of Guangdong Province with grant ID 2024A1515010213.

The authors would like to thank Prof. Yu-Chih Huang of National Yang Ming Chiao Tung University for his fruitful discussions.

REFERENCES

[1] R. Bose and D. Ray-Chaudhuri, "On a class of error correcting binary group codes," *Inf. and Contr.*, vol. 3, no. 1, pp. 68–79, 1960.

[2] A. Hocquenghem, "Codes correcteurs d'erreurs. chiffres (paris), 2, 147-156," *Math. Rev*, vol. 22, p. 652, 1959.

[3] H. Ma and J. Wolf, "On tail biting convolutional codes," *IEEE Trans. Commun.*, vol. 34, no. 2, pp. 104–111, 1986.

[4] E. Arikan, "Channel polarization: A method for constructing capacity-achieving codes for symmetric binary-input memoryless channels," *IEEE Trans. Inf. Theory*, vol. 55, no. 7, pp. 3051–3073, 2009.

[5] K. Niu and K. Chen, "CRC-aided decoding of polar codes," *IEEE Commun. Lett.*, vol. 16, no. 10, pp. 1668–1671, Oct. 2012.

[6] I. Tal and A. Vardy, "List decoding of polar codes," *IEEE Trans. Inf. Theory*, vol. 61, no. 5, pp. 2213–2226, 2015.

[7] E. Arıkan, "From sequential decoding to channel polarization and back again," *preprint available as arXiv:1908.09594*, aug. 2019.

[8] I. Márquez-Corbella and J. Tillich, "Attaining capacity with iterated $(\mathrm{U}|\mathrm{U}+\mathrm{V})$ codes based on AG codes and Koetter-Vardy soft decoding," in *IEEE Int. Symp. Inf. Theory (ISIT)*, Aachen, Germany, 2017, pp. 6–10.

[9] J. Cheng and L. Chen, "BCH based U-UV codes and its decoding," in *IEEE Int. Symp. Inf. Theory (ISIT)*, Melbourne, Australia, 2021, pp. 1433–1438.

[10] W. Chen, J. Cheng, C. Wu and *et al.*, "BCH based U-UV codes and its SCL decoding," *IEEE Trans. on Signal Process.*, vol. 72, pp. 1286–1300, 2024.

[11] C. Wu, W. Chen and *et al.*, "U-UV coding for bit-interleaved coded modulation," *IEEE Trans. Commun.*, vol. 71, no. 9, pp. 5065–5077, 2023.

[12] M. Plotkin, "Binary codes with specified minimum distance," *IRE Trans. Inf. Theory*, vol. 6, no. 4, pp. 445–450, 1960.

[13] P. Trifonov, "Efficient design and decoding of polar codes," *IEEE Trans. Commun.*, vol. 60, no. 11, pp. 3221–3227, 2012.

[14] W. Chen, L. Chen, J. Lin and *et al.*, "Low complexity successive cancellation list decoding of U-UV codes," *China Commun.*, pp. 1–20, 2024.

[15] C.-Y. Lin, Y.-C. Huang, S.-L. Shieh and *et al.*, "Transformation of binary linear block codes to polar codes with dynamic frozen," *IEEE Open J. Commun. Soc.*, vol. 1, pp. 333–341, 2020.

[16] M. Fossorier and S. Lin, "Soft-decision decoding of linear block codes based on ordered statistics," *IEEE Trans. Inf. Theory*, vol. 41, no. 5, pp. 1379–1396, Sept. 1995.

[17] P. Trifonov and V. Miloslavskaya, "Polar codes with dynamic frozen symbols and their decoding by directed search," in *2013 IEEE Inf. Theory Workshop (ITW)*, 2013, pp. 1–5.

[18] D. Wu, Y. Li, and Y. Sun, "Construction and block error rate analysis of polar codes over AWGN channel based on Gaussian approximation," *IEEE Commun. Lett.*, vol. 18, no. 7, pp. 1099–1102, 2014.

[19] T. Richardson, M. Shokrollahi, and R. Urbanke, "Design of capacity-approaching irregular low-density parity-check codes," *IEEE Trans. Inf. Theory*, vol. 47, no. 2, pp. 619–637, 2001.

[20] S.-Y. Chung, T. Richardson, and R. Urbanke, "Analysis of sum-product decoding of low-density parity-check codes using a Gaussian approximation," *IEEE Trans. Inf. Theory*, vol. 47, no. 2, pp. 657–670, 2001.

[21] A. Balatsoukas-Stimming, M. B. Parizi, and A. Burg, "LLR-based successive cancellation list decoding of polar codes," *IEEE Trans. Signal Process.*, vol. 63, no. 19, pp. 5165–5179, 2015.